A Family of High Frequency AC-LED Drivers Based on ZCS-QRCs

Ignacio Castro, *Student Member, IEEE*, Diego G. Lamar, *Member, IEEE*, Sergio Lopez, Kevin Martin, *Student Member, IEEE*, Manuel Arias, *Member, IEEE*, and Javier Sebastian, *Senior Member, IEEE*

***Abstract*—A family of dimmable ac light-emitting-diode (LED) drivers fed from dc voltages, is presented in this paper based on zero-current-switching quasi-resonant converters. The proposed family of drivers is based on replacing the diode in the conventional converter topologies (i.e., buck, boost, or buck–boost) by a string of high-brightness LEDs (HB-LEDs). Hence, the HB-LED string will be working as the rectifier diode and the load, switching at the same frequency of the main switch. In this case, the output current, which is experimentally validated, shows a negative current peak due to the reverse-recovery effect of the HB-LEDs. In order to reduce the reverse-recovery effect on the HB-LEDs, the main switch of the proposed topologies is replaced with a full-wave resonant switch, which makes possible to reduce the d*i*/d*t* during the turn-off of the HB-LED string, therefore the reverse-recovery effect is eliminated. Moreover, the dimming of the HB-LEDs is done by means of changing the switching frequency of the converter by varying the turn-off, while keeping a constant turn-on time. The proposed converters are suggested to be used in a postregulator stage of an ac–dc converter or as the interface between the low-voltage bus and the HB-LED string in a dc nanogrid. In order to validate the analysis, the proposed topologies have been experimentally tested on a constructed prototype with an output power of 7.5 W, that is able to achieve an electrical efficiency of 94.5% and a luminous efficacy of 110 lm/W at full load. Moreover, the analysis has been extended to a comparison in terms of reliability with the conventional topologies on a 700-h test.**

***Index Terms*—AC light-emitting diode (LED), boost, buck–boost, LED driver, zero-current-switching quasi-resonant converters (ZCS-QRC).**

I. Introduction

HIGH-BRIGHTNESS light-emitting diodes (HB-LEDs) are increasingly becoming our main source of the artificial light in our homes, offices, or streets due to their reliability, long life, luminous efficacy, and low maintenance requirements.

Manuscript received August 3, 2017; revised October 11, 2017; accepted November 21, 2017. Date of publication December 6, 2017; date of current version July 15, 2018. This work was supported in part by the Spanish Government under Project MINECO-13-DPI2013-47176-C2-2-R, in part by the Principality of Asturias under Grant "Severo Ochoa" BP14-140 and Grant BP14-85, Project FC-15-GRUPIN14-143, and Project SV-PA-17-RIS3-4, and in part by the European Regional Development Fund (ERDF) grants. Recommended for publication by Associate Editor Dr. M. Ponce-Silva. *(Corresponding author: Ignacio Castro.)*

The authors are with the Departamento de Ingeniería Eléctrica, Electrónica, de Computadores y Sistemas, University of Oviedo, Gijón 33204, Spain (e-mail: castroignacio@uniovi.es; gonzalezdiego@uniovi.es; UO229652@uniovi.es; martinkevin@uniovi.es; ariasmanuel@uniovi.es; sebas@uniovi.es).

Color versions of one or more of the figures in this paper are available online at http://ieeexplore.ieee.org.

Digital Object Identifier 10.1109/TPEL.2017.2780234

However, HB-LEDs are diodes, which means that the current is able to go through them in only one direction. This feature has made the driving of HB-LEDs from the mains an important research topic in a wide range of power [1]. For this reason, it is required the use of an ac–dc converter that feeds the string of HB-LEDs with either a constant [2] or a low-frequency pulsed current in the range of hundreds to thousands of kHz [3]. In fact, for output powers higher than 25 W, it needs to be able to achieve power factor correction (PFC) [4]. Traditionally, an ac–dc HB-LED driver, when cost is not the main concern and reliability and efficiency are of more importance, uses a two-stage [5] or three-stage [6] approach. In fact, the last stage of the driver (i.e., second or third stage) is normally used for the sole purpose of dimming the HB-LEDs, which is traditionally done by lowering the mean value of the output current. In this case, that last stage is also referred as a postregulator. This postregulator stage needs to be cheap and achieve both high efficiency and high power density [7]–[10].

The idea presented in this paper is based on using the basic dc–dc converter topologies (i.e., buck, boost, and buck–boost), which are depicted in Fig. 1(a), (d), and (g) and replace their diode D_1 with the string of HB-LEDs while short circuiting their output. As a result, two different converters can be obtained: LED paralleled with switch (DL//S, i.e., Fig. 1(e)) and LED paralleled with inductor (DL//*L*, i.e., Fig. 1(b) and (h)). It should be noted, that while in the conventional buck, boost, and buck–boost converters, the HB-LEDs are supplied with a constant current, in DL//S and DL//*L*, the HB-LED string is supplied with a pulsed current, pulsing at the same frequency as the main switch (i.e., S_1). The operation of HB-LEDs at high frequencies (i.e., $>$100 kHz) acting as the regular diodes of a power converter, also referred in the literature as high-frequency ac-LED driving, has been studied by means of resonant dual half bridges applying a sinusoidal high-frequency current waveform to the HB-LEDs [11]–[13], a flyback converter working in discontinuous conduction mode [14] and self-oscillating topologies [15]. However, there is no factual evidence on how will the HB-LEDs perform under a high-frequency sinusoid or triangular current waveform in terms of light quality, reliability, or correlated color temperature (CCT).

Following the same principle, some studies have been dedicated to the driving of white HB-LEDs (i.e., pulsewidth modulation dimming) under different current waveforms (i.e., sinusoidal, square, and triangular) at 50 Hz [16] or up to 1 MHz with square waveforms [17], [18]. Some important

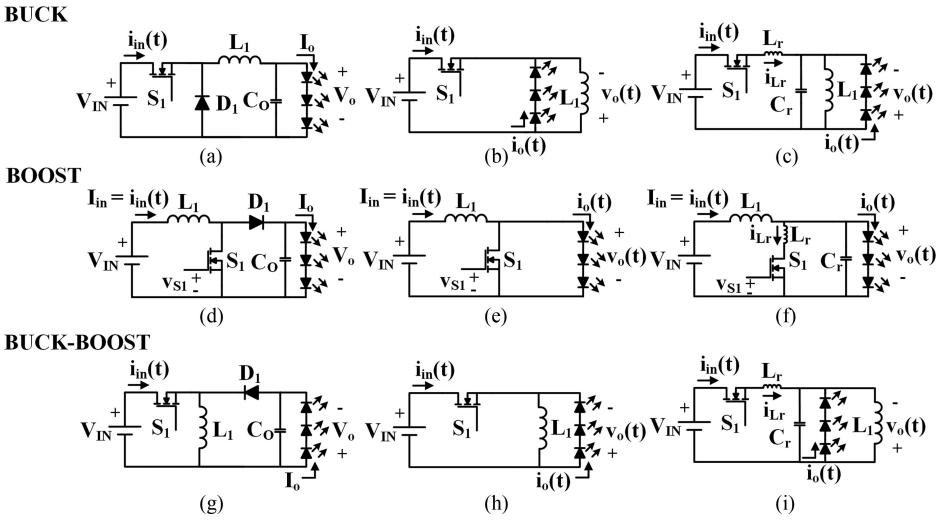

Fig. 1. Basic converters. (a) Buck converter. (b) DL//*L* converter. (c) DL//*L* ZCS-QRC. (d) Boost converter. (e) DL//S converter. (f) DL//S ZCS-QRC. (g) Buck–boost converter. (h) DL//*L* converter. (i) DL//*L* ZCS-QRC.

conclusions can be extracted from these works. First, the increase of frequency in a square current waveform from 100 Hz to 300 kHz does not have a negative impact on either the junction temperature or the light efficiency. Second, pulsed current is actually better for white HB-LEDs in terms of degradation over time. Third, the pulsed current technique is also regarded as a better driving technique than constant current in terms of chromaticity shifts [19]. And fourth, the switching of HB-LEDs at higher frequencies than 3 kHz presents no visible flicker or harmful effects to the viewers [20].

Regarding the previous facts, it is necessary to understand how well would an HB-LED operate as a diode due to the lack of dynamic characterization in the manufacturer datasheets of white HB-LEDs. In the previous literature, some studies have characterized the frequency response of white HB-LEDs for visible light communications [21], showing a bandwidth of up to 3 MHz for regular white light. However, this study does not add any information on how fast can the LED truly switch. Therefore, a study to characterize the HB-LED string under high-frequency switching operation in power converters is required to observe, whether the well-known phenomena of reverse recovery [22] could occur in the proposed topologies when an HB-LED is used as the rectifier of the converter. Considering that the reverse-recovery effect could occur on the HB-LEDs, the d*i*/d*t* during the turn-off of the HB-LED needs to be lowered to diminish its effects or even eliminate it. The d*i*/d*t* reduction can be performed by either increasing the count of switches [23], which is not desirable, or by means of a zero-current-switched quasi-resonant converter (ZCS-QRC). This last fact is achieved in ZCS-QRCs, whose main characteristic is achieving zero-current switching (ZCS) on the main switch, due to the inclusion of an inductor in the path of the main switch that causes the current through the rectifier to diminish steadily to the zero value. The ZCS-QRC equivalent will be obtained by replacing the main switch of DL//*L* and DL//S with the full-wave resonant switch [24]–[26]. This renders two converters: DL//*L* ZCS-QRC [i.e., Fig. 1(c) and (i)] and DL//S ZCS-QRC [i.e., Fig. 1(f)].

The proposal of this paper is for these converters to be used as a postregulator when driving HB-LEDs from the mains or as the required interface between the low-voltage bus and one of the several strings of HB-LEDs that can be present in a dc nanogrid [28]. Moreover, the dimming of the HB-LEDs is done by means of changing the switching frequency of the converter, by varying the turn-off and keeping a constant turn-on time in the main switch.

Summarizing, this paper analyses the working principle, from a static point of view, for both proposed topologies: DL//*L* ZCS-QRC and DL//S ZCS-QRC, which is carried out in Section II. Furthermore, in order to validate the analysis carried out in Section II, two prototypes based on the two proposals of this paper have been constructed an experimentally tested and its results have been summarized in Section III. In this section, the results of a reliability test that has been carried out for 700 h comparing a conventional boost, a DL//S and a DL//S ZCS-QRC are also summarized. Finally, some conclusions are discussed in Section IV from the aforementioned experimental results.

II. Working Principle

The concept of the dc–dc HB-LED drivers presented in this paper is based on using the HB-LEDs as the rectifier diode of a dc–dc converter with a full-wave resonant switch. The main reason for using a full-wave resonant switch, is based on one of the key characteristics that this driver needs to have, which is the ability to achieve full dimming. It is a well-known fact that the input/output relationship of a half-wave ZCS-QRC varies greatly with the load. In a driver in which the output current will be varying from zero to maximum current to meet the driving requirements, this fact will complicate unnecessarily its control. Hence, this analysis is only going to be considered for full-wave resonant switches that are invariable with its load.

In the forthcoming analysis, the HB-LEDs are considered to be an ideal diode in series with their dynamic resistance (r_{LED})

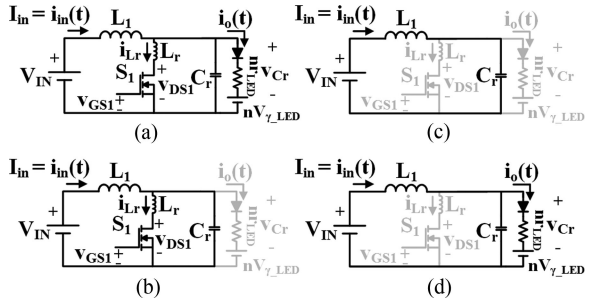

Fig. 2. Equivalent circuits of the proposed DL//S ZCS-QRC. (a) $[t_0, t_1]$ linear stage. (b) $[t_1, t_2]$ resonant stage. (c) $[t_2, t_3]$ delay stage. (d) $[t_3, t_4]$ lighting stage.

and their forward voltage $(V_{\gamma\_\mathrm{LED}})$. Moreover, the MOSFET (S_1) will be considered as an ideal switch. It is also important to note that the main inductor (L_1) is going to be considered much larger than the resonant inductor (L_r) in order for L_1 not to affect the resonant frequency between L_r and the resonant capacitor (C_r), which is a well-known fact in ZCS-QRCs [24]. Moreover, in the case of the proposed topology, L_1 needs to be large enough to satisfy that the current ripple is also as small as possible. Hence, being able to consider the output current as constant during the conduction of the HB-LEDs. This reason makes the increase of the switching frequency an attractive solution to diminish the size of L_1, which will be the most limiting factor in terms of size in the proposed driver.

The resonant tank comprised by L_r and C_r, will resonate at

$$\omega_n = \frac{1}{\sqrt{L_r C_r}} \tag{1}$$

and the characteristic impedance is defined by

$$Z_n = \sqrt{\frac{L_r}{C_r}}. \tag{2}$$

A. Static Analysis of the DL//S ZCS-QRC

The operation of the HB-LED driver is summarized in Fig. 2, where the four equivalent circuits that the DL//S ZCS-QRC undergoes during its operation are depicted. Fig. 3 shows the most representative waveforms for said topology with the same time basis as Fig. 2.

1) Linear Stage [t_0, t_1], Fig. 2(a): Coming from the lighting stage Fig. 2(d), in which the HB-LED string is supplied with a constant current, this stage starts when $\mathrm{S_1}$ is turned ON. At the time $\mathrm{S_1}$ is turned ON, $\mathrm{i_{Lr}}$ will start increasing steadily and $\mathrm{i_o}$ will decrease accordingly with the same slope, until it reaches the zero current value.

The initial conditions for this stage will be $\mathrm{i_o}(0) = \mathrm{I_{in}}, \mathrm{i_{Lr}}(0) = 0$, and $\mathrm{v}_{Cr}(0) = \mathrm{V_o}$, where $\mathrm{V_o}$ is the maximum output voltage obtained during the freewheeling stage, being the state equations of this stage defined as

$$\begin{cases} I_{\mathrm{in}} = i_{L_r}(t) + C_r \frac{dv_{C_r}(t)}{dt} + i_o(t) \\ v_{C_r}(t) = i_o(t) n r_{\mathrm{LED}} + n V_{\gamma\_\mathrm{LED}} \\ L_r \frac{di_{L_r}(t)}{dt} = v_{C_r}(t) \end{cases} \tag{3}$$

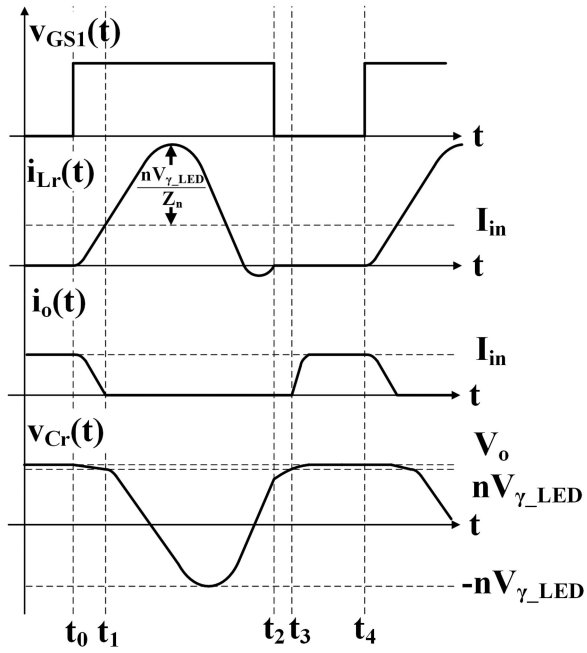

Fig. 3. Most representative time-domain waveform for DL//S ZCS-QRC.

where n represents the number of HB-LEDs in series on the string, I_{in} represents the input current considered as a constant due to the larger value of L_1, $i_{Lr}(t)$ is the current through L_r, $i_o(t)$ is the current through the HB-LED string, $v_{Cr}(t)$ is the voltage that the HB-LEDs will withstand, and V_o is the voltage withstood by the HB-LEDs during their conduction.

By solving (3), the analytical waveforms for this stage can be obtained as

$$v_{C_r}(t) = \left(\frac{I_{\mathrm{in}} r_{\mathrm{LED}} + V_{\gamma_{\mathrm{LED}}}}{r_{\mathrm{LED}} C_r}\right) A(t) + V_o B(t) \tag{4}$$

$$i_{L_r}(t) = \frac{V_o}{L_r} A(t) + \left(\frac{I_{\mathrm{in}} r_{\mathrm{LED}} + V_{\gamma_{\mathrm{LED}}}}{r_{\mathrm{LED}} C_r}\right) C(t) \tag{5}$$

where $A(t)$, $B(t)$, and $C(t)$ are defined as follows:

$$A(t) = \frac{1}{2\omega_n \sqrt{\xi^2 - 1}} \left(e^{-\left(\xi - \sqrt{\xi^2-1}\right)\omega_n t} - e^{-\left(\xi + \sqrt{\xi^2-1}\right)\omega_n t} \right) \tag{6}$$

$$B(t) = \frac{1}{2\sqrt{\xi^2 - 1}} \left[\left(\xi + \sqrt{\xi^2 - 1}\right) e^{-\left(\xi + \sqrt{\xi^2-1}\right)\omega_n t} - \left(\xi - \sqrt{\xi^2 - 1}\right) e^{-\left(\xi - \sqrt{\xi^2-1}\right)\omega_n t} \right] \tag{7}$$

$$C(t) = 1 + \frac{1}{2\sqrt{\xi^2 - 1}} \left[\left(\xi - \sqrt{\xi^2 - 1}\right) e^{-\left(\xi + \sqrt{\xi^2-1}\right)\omega_n t} - \left(\xi + \sqrt{\xi^2 - 1}\right) e^{-\left(\xi - \sqrt{\xi^2-1}\right)\omega_n t} \right] \tag{8}$$

where ξ is defined by

$$\xi = \frac{1}{2 r_{\mathrm{LED}}} \sqrt{\frac{L_r}{C_r}}. \tag{9}$$

From (3) and (4), $i_o(t)$ can be derived, which can then be used to determine the duration of this stage since it finishes when $i_o(t)$ reaches the zero value. However, it would be unpractical to use (4) and (5) in this calculation. Hence, an approximation can be obtained by considering $v_{Cr}(t)$ as a constant voltage, since during this stage, the voltage on the HB-LED string diminishes until it reaches nV_{γ_LED}, as shown in Fig. 3.

By using this approximation, (3) can be simplified to

$$L_r \frac{di_{L_r}(t)}{dt} = V_o \tag{10}$$

$$i_o(t) = I_{\mathrm{in}} - i_{L_r}(t). \tag{11}$$

Combining (10) and (11), the duration of this stage can be yielded

$$t_1 - t_0 = \frac{L_r I_{\mathrm{in}}}{V_o}\ . \tag{12}$$

As can be seen the value of L_r controls the duration of this stage, hence, controlling the d*i*/d*t* of i_o. Therefore, with an adequate selection of the value for L_r, the effects of the reverse recovery caused by the HB-LEDs due to their operation as rectifiers in the proposed topology can be diminished or even eliminated. Therefore, this stage is key for the correct operation of the proposed driver and (12) marks the first design criteria for the current driver, which will define the minimum the value of L_r.

2) Resonant Stage [t_1, t_2], Fig. 2(b): This stage starts when the HB-LEDs are turned OFF and finishes in a resonant period when $\mathrm{S_1}$ is turned OFF. However, when the current on $\mathrm{i_{Lr}}$ becomes negative, the switch no longer controls the flow of the current, as the parasitic diode is the one in control causing inaccuracies to occur in terms of the on time. If that were the case, the stage will finish when the current reaches the zero value. The state equations are similar to the boost ZCS-QRC [24], and are defined by

$$\begin{cases} L_r \frac{di_{L_r}(t)}{dt} = v_{C_r}(t) \\ C_r \frac{dv_{C_r}(t)}{dt} = I_{\mathrm{in}} - i_{L_r}(t) \end{cases} \tag{13}$$

with the next initial conditions: $v_{Cr}(t_1) = nV_{\gamma\_\mathrm{LED}}$ and $i_{Lr}(t_1)$ derived from (5) at the end of the last stage.

From (13), the waveforms of the most important variables can be derived as

$$i_{L_r}(t) = I_{\mathrm{in}} + \frac{nV_{\gamma_{\mathrm{LED}}}}{Z_n} \sin(\omega_n t) + (i_{L_r}(t_1) - I_{\mathrm{in}}) \cos(\omega_n t) \tag{14}$$

$$v_{C_r}(t) = nV_{\gamma_{\mathrm{LED}}} \cos(\omega_n t) - Z_n (i_{L_r}(t_1) - I_{\mathrm{in}}) \sin(\omega_n t). \tag{15}$$

The duration of this stage can be approximated by

$$t_2 - t_1 = \frac{\alpha}{\omega_n} \tag{16}$$

considering that $(i_{L_r}(t_1) - I_{\mathrm{in}})$ is negligible when compared to the other terms in (15) and where α can be defined as

$$\alpha = \arcsin\left(\frac{-I_{\mathrm{in}} Z_n}{nV_{\gamma_{\mathrm{LED}}}}\right), \frac{3\pi}{2} < \alpha < 2\pi. \tag{17}$$

3) Delay Stage [t_2, t_3], Fig. 2(c): During this stage, $\mathrm{C_r}$ keeps being charged until $\mathrm{v_{Cr}(t)}$ reaches nV_{γ_LED}, which marks the end of this stage. The initial conditions for $\mathrm{v_{Cr}(t)}$ is set by the previous stage as $\mathrm{v_{Cr}(t_2)}$. This stage can be defined by

$$C_r \frac{dv_{C_r}(t)}{dt} = I_{\mathrm{in}}. \tag{18}$$

Hence, C_r gets charger following the next expression:

$$v_{C_r}(t) = \frac{I_{\mathrm{in}}}{C_r}\, t + v_{C_r}(t_2). \tag{19}$$

C_r is being charged lineally, and the time this stage lasts can be yield as follows:

$$t_3 - t_2 = \frac{C_r (nV_{\gamma_{\mathrm{LED}}} - v_{C_r}(t_2))}{I_{\mathrm{in}}} \tag{20}$$

which means that the higher the value of C_r the longer it will take the HB-LEDs to start illuminating. Therefore, (20) marks another key equation in the design of the driver under study.

4) Lighting Stage [t_3, t_4], Fig. 2(d): Having reached $v_{Cr}(t_3) = nV_{\gamma\_\mathrm{LED}}$, at the end of the delay stage, the HB-LEDs start turning ON during this stage as their current increases. The state equations for this stage are

$$\begin{cases} I_{\mathrm{in}} = i_o(t) + C_r \frac{dv_{C_r}(t)}{dt} \\ v_{C_r}(t) = i_o(t) n r_{\mathrm{LED}} + nV_{\gamma\_\mathrm{LED}}. \end{cases} \tag{21}$$

From the aforementioned equation, the next expressions can be derived

$$v_{C_r}(t) = I_{\mathrm{in}}\ nr_{\mathrm{LED}} \left(1 - e^{-\frac{1}{nr_{\mathrm{LED}} C_r} t}\right) + nV_{\gamma\_\mathrm{LED}} \tag{22}$$

$$i_o(t) = I_{\mathrm{in}} \left(1 - e^{-\frac{1}{nr_{\mathrm{LED}} C_r} t}\right) \tag{23}$$

where it can be seen that $i_o(t)$ increases exponentially until it reaches I_{in}. The time it takes to reach I_{in} can be approximated by

$$t_d - t_3 = 5nr_{\mathrm{LED}} C_r \tag{24}$$

considering that it will take five times the time constant to reach said value, which is completely dependent of C_r. Here, (24) is a key equation in the selection of C_r, and the designer needs to use the most restrictive of (20) and (24) in the design. This stage will end when $\mathrm{S_1}$ is turned ON again, hence, entering once more in the linear stage.

After the thorough analysis carried out for the four stages that comprise the full operation of the ZCS-QRC DL//S, a relationship needs to be established between the input, and the output current, to understand how this driver is controlled. For that reason, the average value of $i_o(t)$ is going to be calculated by integrating $i_o(t)$ in the whole switching period, considering for practical reasons that the linear and the delay stages are negligible, when compared to the duration of the resonant and the lighting stages. Hence

$$I_o = \frac{1}{T_s} \int_0^{T_s - T_n} i_o(t) dt = I_{\mathrm{in}} \left(\frac{T_s - T_n}{T_s} - \frac{nr_{\mathrm{LED}} C_r}{T_s}\right) \tag{25}$$

where I_o is the average value of the output current, T_s is the switching period, and T_n is the resonant period. In (25),

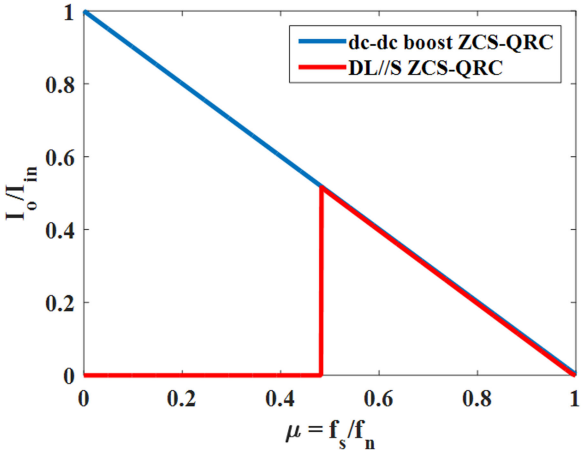

Fig. 4. Comparison of $I_o/I_{\rm in}$ versus μ, for the dc–dc boost ZCS-QRC and DL//S ZCS-QRC.

$nr_{\rm LED}C_r$ defines the time constant of the lighting stage, see Fig. 2(c), whose value can be considered negligible. Therefore

$$I_o = I_{\rm in}\,(1-\mu) \tag{26}$$

where μ is the control variable of the driver defined by

$$\mu = \frac{T_n}{T_s} = \frac{f_s}{f_n} \tag{27}$$

where f_s is the switching frequency and f_n is the resonant frequency. From this analysis, it can be seen that the driver can control I_o by varying the switching frequency while keeping a constant on-time (t_{on}), similarly to a conventional dc–dc boost ZCS-QRC. Fig. 4 shows a comparison between the dc–dc boost ZCS-QRC and the DL//S ZCS-QRC, in terms of the relationship between I_o and $I_{\rm in}$, versus μ. As can be seen, the behavior of the proposed driver is similar to the dc–dc boost ZCS-QRC until it reaches a certain value of μ at which the driver is not able to enter in the lighting stage due to the inability of $v_{Cr}(t)$ to reach $nV_{\gamma\_\rm LED}$, hence not being able to turn-on the HB-LED string. A real scenario is used for this comparison, with the minimum μ at which the driver is not able to supply current to the HB-LEDs being dependent on the $nV_{\gamma\_\rm LED}$ of the selected string and on the design specifications of the driver.

The last part of this analysis is to study the condition that guarantees the ZCS of the proposed driver so that the switch can be turned OFF during this time. For that reason, (17) needs to be studied to attain the values that give valid solutions of the arcsine in the range under study to achieve that the current is zero on $i_{Lr}(t)$ at instant t_2. Hence, yielding

$$\frac{nV_{\gamma_{\rm LED}}}{Z_n} \geq I_{\rm in}. \tag{28}$$

B. Static Analysis of the DL//L ZCS-QRC

Similarly, the analysis is carried out for the DL//S ZCS-QRC; this subsection will analyze in detail the operation of the DL//L ZCS-QRC. The current through L_1 will also be considered

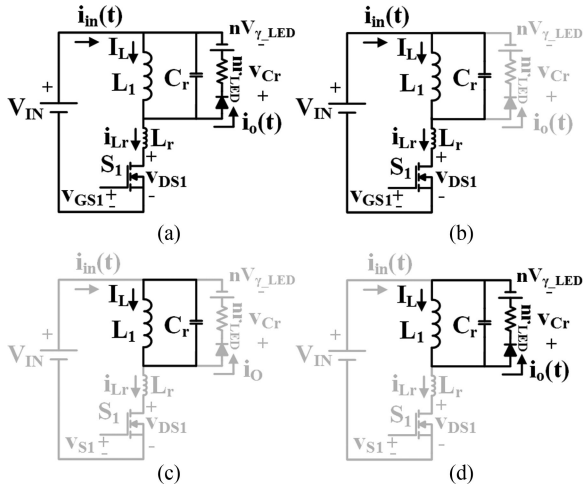

Fig. 5. Equivalent circuits of the proposed DL//L ZCS-QRC. (a) $[t_0, t_1]$ linear stage. (b) $[t_1, t_2]$ resonant stage. (c) $[t_2, t_3]$ delay stage. (d) $[t_3, t_4]$ lighting stage.

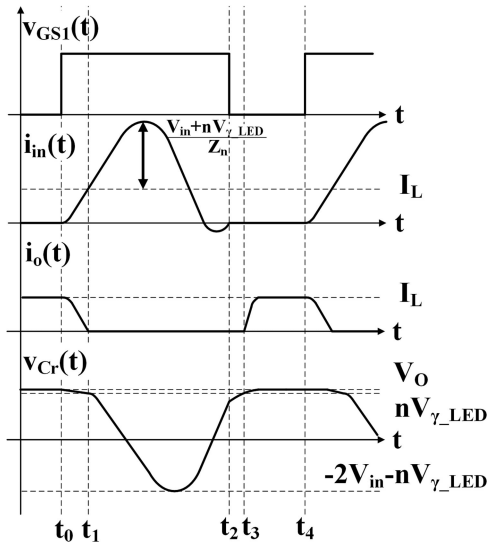

Fig. 6. Most representative time-domain waveform for the DL//S ZCS-QRC.

constant (I_L) as the inductor will be selected to be much larger than L_r and to also have as little ripple as possible.

It should also be noted, that the topology selected to carry out this subsection is not the one depicted in Fig. 2(c) and (i), but an equivalent with its main switch referred to the ground of the input voltage. The main reason for this change, is to simplify the driving of the main switch, which is possible since the load of the converter is based on an HB-LED string.

The four equivalent circuits that this driver undergoes during its operation, are depicted in Fig. 5. Furthermore, the most representative waveforms to correctly exemplify its operation are presented in Fig. 6, sharing the same time basis as the equivalent circuits of Fig. 5. From Figs. 5 and 6, it can be seen that the converter operates similarly to the DL//S ZCS-QRC.

1) Linear Stage $[t_0, t_1]$, Fig. 5(a): Coming from the free-wheeling stage, see Fig. 5(d), in which the HB-LED string is supplied with a constant current, this stage begins when S_1 is

turned ON. At that time, $\mathrm{i}_{in}(\mathrm{t})$ will start increasing steadily and $\mathrm{i}_{\mathrm{o}}(\mathrm{t})$ will decrease accordingly with the same slope, until it reaches the zero current value.

The initial conditions for this stage will be $i_o(0) = I_L, i_{Lr}(0) = 0$, and $v_{Cr}(0) = V_o$. Hence, the state equations of this stage are defined by

$$\begin{cases} C_r \frac{dv_{C_r}(t)}{dt} = -i_{\mathrm{in}}(t) + I_L - i_o(t) \\ v_{C_r}(t) = i_o(t) n r_{\mathrm{LED}} + n V_{\gamma\_\mathrm{LED}} \\ L_r \frac{di_{\mathrm{in}}(t)}{dt} = V_{\mathrm{in}} + v_{C_r}(t). \end{cases} \tag{29}$$

By solving the aforementioned equation, the analytical waveforms for this stage can be derived as

$$v_{C_r}(t) = V_{\mathrm{in}} + \left(I_L + \frac{n V_{\gamma_{\mathrm{LED}}} - V_{\mathrm{in}}}{n r_{\mathrm{LED}} C_r} \right) A(t) - (V_{\mathrm{in}} + V_o) B(t) \tag{30}$$

$$i_{\mathrm{in}}(t) = \frac{V_{\mathrm{in}} + V_o}{L_r} A(t) - \left(I_L + \frac{n V_{\gamma_{\mathrm{LED}}} - V_{\mathrm{in}}}{n r_{\mathrm{LED}} C_r} \right) C(t). \tag{31}$$

In a similar fashion to what was done in the last subsection during the linear stage, $v_{Cr}(t)$ will be considered constant to obtain a practical estimation of the duration of this stage. Hence, the state equations can be presented as

$$\begin{cases} I_L = i_{\mathrm{in}}(t) + i_o(t) \\ L_r \frac{di_{\mathrm{in}}(t)}{dt} = V_{\mathrm{in}} + V_o. \end{cases} \tag{32}$$

From the aforementioned equation, the duration of this stage can be yielded by obtaining $i_o(t)$, and then, solving the equation for $i_o(t_1) = 0$. Hence

$$t_1 - t_0 = \frac{L_r I_L}{V_{\mathrm{in}} + V_o}. \tag{33}$$

As the aforementioned equation shows, the value of L_r controls the duration of this stage in a similar fashion to the one explained in the previous subsection for the DL//S ZCS-QRC.

2) Resonant Stage [t_1, t_2], Fig. 5(b): This stage starts when the HB-LED string is turned OFF and it finishes in a resonant period when S_1 is turned OFF. The state equations are defined by

$$\begin{cases} L_r \frac{di_{L_r}(t)}{dt} = v_{C_r}(t) \\ C_r \frac{dv_{C_r}(t)}{dt} = I_L - i_{L_r}(t) \end{cases} \tag{34}$$

with its initial conditions being: $v_{Cr}(t_1) = nV_{\gamma\_\mathrm{LED}}$ and $i_{\mathrm{in}}(t_1)$ derived from (31) at the end of the last stage.

From (34), the waveforms of the most important variables can be derived as follows:

$$i_{L_r}(t) = I_L + \frac{V_{\mathrm{in}} + n V_{\gamma_{\mathrm{LED}}}}{Z_n} \sin(\omega_n t) + (i_{L_r}(t_1) - I_L) \cos(\omega_n t) \tag{35}$$

$$v_{C_r}(t) = V_{\mathrm{in}} - (V_{\mathrm{in}} + n V_{\gamma_{\mathrm{LED}}}) \cos(\omega_n t) + Z_n (i_{L_r}(t_1) - I_L) \sin(\omega_n t) \tag{36}$$

The duration of this stage can be approximated by

$$t_2 - t_1 = \frac{\beta}{\omega_n} \tag{37}$$

considering that $(i_{in}(t_1) - I_L)$ is negligible when compared to the other terms in (35), and where β can be defined by

$$\beta = \arcsin\left(\frac{-I_L Z_n}{V_{\mathrm{in}} + n V_{\gamma_{\mathrm{LED}}}} \right), \quad \frac{3\pi}{2} < \alpha < 2\pi. \tag{38}$$

It should be noted that during this stage the HB-LED string will withstand a negative voltage, which in the case of the DL//S ZCS-QRC was equal to the $n{\cdot}V_{\gamma\_\mathrm{LED}}$. However, in the DL//*L* ZCS-QRC is $2V_{\mathrm{in}} + nV_{\gamma\_\mathrm{LED}}$, as shown by (36). According to manufacturers, HB-LEDs are able to withstand a negative voltage equal to nV_{γ_LED}, which complies in the case of the DL//S ZCS-QRC but not in the one currently under study [29].

3) Delay Stage [t_2, t_3], Fig. 5(c): In this stage, $\mathrm{C_r}$ continuously charges until $\mathrm{v_{Cr}(t)}$ reaches nV_{γ_LED}, which marks the end of this stage. The initial conditions for $\mathrm{v_{Cr}(t)}$ is set by the previous stage as $\mathrm{v_{Cr}(t_2)}$. This stage can be defined by

$$C_r \frac{dv_{C_r}(t)}{dt} = I_L. \tag{39}$$

Hence, C_r gets charger following the next expression:

$$v_{C_r}(t) = \frac{I_L}{C_r} t + v_{C_r}(t_2). \tag{40}$$

C_r is being charged lineally, and the time this stage lasts can be yield from (41) as

$$t_3 - t_2 = \frac{C_r (n V_{\gamma_{\mathrm{LED}}} - v_{C_r}(t_2))}{I_{\mathrm{in}}} \tag{41}$$

which follows the same principle as the one presented for the which follows the same principle as the one presented for the previous driver.

4) Lighting Stage [t_3, t_4], Fig. 5(d): Having reached $v_{Cr}(t_3) = n \cdot V_{\gamma\_\mathrm{LED}}$, the HB-LEDs start illuminating. The state equations that define this stage are summarized as

$$\begin{cases} I_L = i_o(t) + C_r \frac{dv_{C_r}(t)}{dt} \\ v_{C_r}(t) = i_o(t) n r_{\mathrm{LED}} + n V_{\gamma\_\mathrm{LED}}. \end{cases} \tag{42}$$

From the aforementioned equation, the next expressions can be derived as

$$v_{C_r}(t) = I_L\, n r_{\mathrm{LED}} \left(1 - e^{-\frac{1}{n r_{\mathrm{LED}} C_r} t} \right) + n V_{\gamma\_\mathrm{LED}} \tag{43}$$

$$i_o(t) = I_L \left(1 - e^{-\frac{1}{n r_{\mathrm{LED}} C_r} t} \right) \tag{44}$$

where it can be seen that $i_o(t)$ increases exponentially until it reaches I_L. The time it takes to reach I_L can then be approximated by (24). Hence, (24) and (42) are key equations for the selection of C_r. This stage will end when the switch S_1 is turned ON again, hence, starting the linear stage.

If the same considerations are done in the previous section to calculate $i_o(t)$, then by integrating (44) in a switching period,

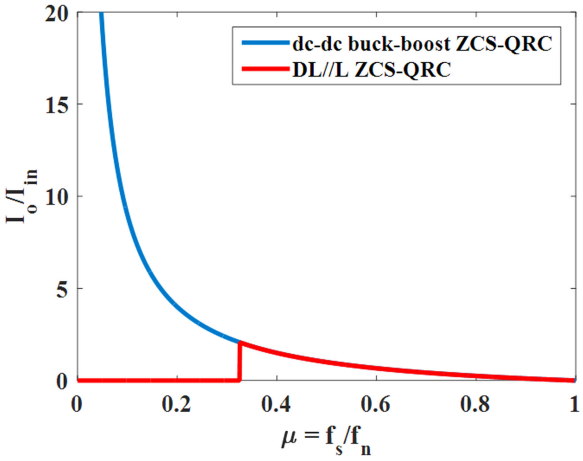

Fig. 7. Comparison of $I_o/I_{\rm in}$ versus μ, for the dc–dc buck–boost ZCS-QRC and DL//*L* ZCS-QRC.

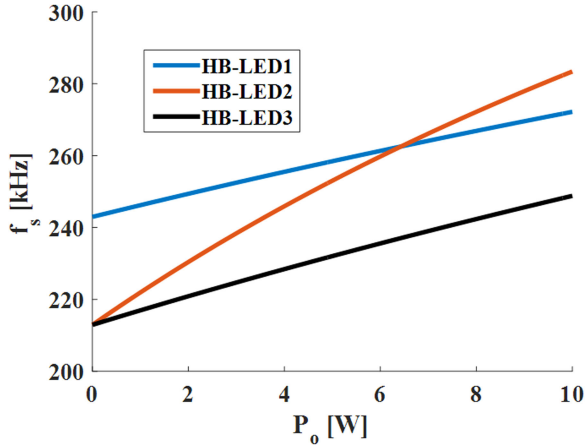

Fig. 8. Comparison of f_s versus P_o, for three different commercial HB-LEDs as a load of the DL//S ZCS-QRC.

I_o can be obtained as

$$I_o = \frac{1}{T_s}\int_0^{T_s-T_n} i_o(t)dt = I_L\left(\frac{T_s-T_n}{T_s} - \frac{nr_{\rm LED}C_r}{T_s}\right). \tag{45}$$

From the aforementioned equation, a relationship between I_L and I_o can be obtained. However, it is necessary to relate I_o to the average input current $(I_{\rm in})$, which can be obtained by relating I_L and $I_{\rm in}$. Keeping in mind the considerations made

$$I_{\rm in} = I_L\frac{T_n}{T_s}. \tag{46}$$

Taking into account that, $nr_{\rm LED}C_r$ can be considered negligible in comparison to the resonant and lighting stage, the next expression can be obtained as

$$I_o = I_{\rm in}\frac{(1-\mu)}{\mu}. \tag{47}$$

From this analysis, it can be seen that the driver can be controlled by varying the switching frequency while keeping $t_{\rm on}$ constant, similarly to the DL//S ZCS-QRC introduced in the previous subsection. Fig. 7, shows a comparison between of a conventional dc–dc buck–boost ZCS-QRC and the DL//*L* ZCS-QRC, in terms of the ratio $I_o/I_{\rm in}$ as a function of μ, where it can be seen that the behavior of the proposed driver is similar to the conventional dc–dc buck–boost ZCS-QRC. However, this happens from a certain value of μ at which the driver is able to enter in the lighting stage, since it is capable of reaching $nV_{\gamma\perp{\rm LED}}$ on $v_{Cr}(t)$. Hence, being able to illuminate the HB-LED string.

The last part of this analysis is to study which condition guarantees that the proposed driver achieves ZCS so that the switch can be turned OFF during this time. For that reason, (38) needs to be studied to obtain the values that make the arcsine valid in the range under study while achieving zero current on $i_{\rm in}(t)$ at instant t_2. Hence, yielding

$$\frac{V_{\rm in}+nV_{\gamma_{\rm LED}}}{Z_n} \geq \frac{I_{\rm in}}{\mu}. \tag{48}$$

TABLE I
CHARACTERISTICS OF HB-LEDS UNDER STUDY

	$V_{\gamma\perp{\rm LED}}[V]$	$r_{\rm LED}[\Omega]$
HB-LED1	2.9	0.44
HB-LED2	2.6	1
HB-LED3	2.6	0.44

C. Design Criteria

The design criteria will only be detailed for the DL//S ZCS-QRC and should follow the same principle for the DL//*L* ZCS-QRC. First, (12) needs to be used with the design requirements to select a value of L_r that guarantees that the time of the linear stage lasts long enough to eliminate the reverse recovery of the diode. This effect is completely reliant on the selected HB-LED, but aiming for a d*i*/d*t* of 500 A/ns can be considered a good design practice for the newer HB-LEDs on the market. Once L_r is selected, a tradeoff needs to be found between (20), (24), and (28). In most scenarios, the most restrictive equation would be (28) that guarantees that ZCS is achieved in the driver. However, if the switching frequency cannot be lowered due to design restrictions, the ZCS condition can be ignored, as this will cause longer times on the delay stage or the settling stage. Hence, causing the HB-LED string to work with higher currents during shorter times to compensate for the longer off times.

Once the driver is designed and f_n is available, it is important to understand how does the driver operate depending on the characteristics of the HB-LED. Fig. 8 shows the frequency range in relation to the output power of the driver for three different HB-LEDs with similar power characteristics, and different $V_{\gamma\perp{\rm LED}}$ and $r_{\rm LED}$, which are summarized in Table I. From Fig. 8, it can be seen that $r_{\rm LED}$ determines the wideness of the frequency range, whereas $V_{\gamma\perp{\rm LED}}$ determines the starting frequency of the driver. In that sense, considering the dependence of the parameter with the junction temperature, the designer should consider $V_{\gamma\perp{\rm LED}}$ at the operating junction temperature to select the starting frequency of the driver.

The last element that needs to be determined for the proposed driver is the main inductance (L_1). The determination

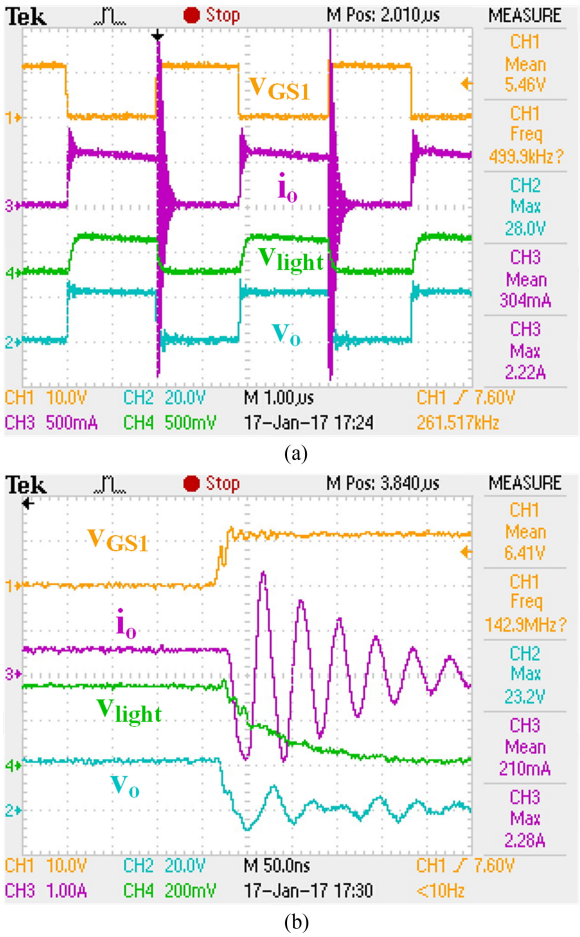

Fig. 9. Most representative waveforms of DL//S. (a) Switching operation. (b) Zoom during the reverse recovery.

of its value can be done by considering that the inductance is magnetized during the on time. Hence, rendering

$$L_1 = \frac{V_{\text{in}}^2}{2P_{\text{in}}\Delta I_{\%} f_n} \tag{49}$$

where $\Delta I_{\%}$ is the percentage ripple of the input current and P_{in} is the input power of the LED driver.

III. Experimental Results

Before tackling the actual design of the drivers, it is necessary to observe whether the HB-LEDs will have a representative reverse-recovery effect when working as the rectifier of a dc–dc converter. For that reason, a DL//S driver has been designed and built for a maximum power of 7.5 W. The most important waveforms of that driver are summarized in Fig. 9 with said driver switching at 500 kHz. As can be seen in Fig. 9(a), the output current $(i_o(t))$ presents an undesirable ringing toward the turn-off. If the area is zoomed, see Fig 9(b), it can be seen that the ringing is caused by the huge reverse recovery effect of the HB-LED string. In order to evaluate the impact of the reverse recovery on the light output generated by the HB-LED string, the light has been measured with a high bandwidth photodiode (S5972) used in conjunction with a transimpedance amplifier [21]. The green signal, represents the voltage measured by the transimpedance

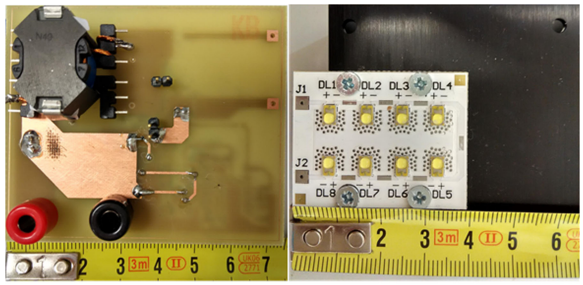

(a) (b)

Fig. 10. Designed and constructed prototype. (a) DL//S ZCS-QRC. (b) HB-LED string of Lumiled LXML-PWC2.

amplifier (v_{light}), which coincides with the light the HB-LED string is supplying. The ringing causes an activation of the HB-LEDs, which makes them to turn-off slower due to their inability to replicate the ringing of i_o. This ringing has a frequency of 24 MHz, that is not replicated because of the bandwidth limitation of the HB-LED string, causing a minimized effect on the generated light. However, even if this effect is not critical in terms of light, it is significant in terms of actual losses causing the HB-LED string to undergo an increase of more than 15 °C when compared with the conventional continuous current scenario. The temperature increase is the main reason why their QRC-ZCS counterparts are proposed to diminish the undesirable effect of reverse recovery.

Therefore, this section summarizes the most important experimental results for both drivers under study, which have been designed and experimentally tested for a maximum power of 7.5 W, feeding eight HB-LEDs (LXML-PWC2). Fig. 10 shows a picture of one of the drivers and one of the HB-LED strings, with their size measured in centimeters. It should be noted, that the size of all the prototypes discussed in this section will coincide with the one showed in Fig. 10(a).

Furthermore, the analysis will be extended for the DL//S ZCS-QRC, as it will be compared to a conventional dc–dc boost, see Fig. 1(d), and the DL//S, see Fig. 1(e), in terms of reliability to correctly study whether the effect of the reverse recovery observed in the DL//S has an actual impact in terms of actual degradation on the HB-LEDs. This comparison requires for the drivers to be working for several hundred hours (i.e., 700 h), which means that in order to assure that I_o is kept constant, a control loop will be required and designed as similar as possible for all the drivers. For the sake of the comparison, all the drivers under test use the same analog integrated circuit (MC33023) in order to diminish the uncertainty that will cause the usage of different controllers, which in the case of the DL//S ZCS-QRC and DL//*L* ZCS-QRC requires some extra circuitry.

A. Experimental Results for the DL//S ZCS-QRC

The DL//S ZCS-QRC has been designed for an input voltage of 12-V feeding a string of eight HB-LEDs, which are equivalent to an output voltage of 24 V at 0.3 mA. Following the design criteria introduced in the previous section, Table II summarizes the components selected in the design, which have been selected to completely eliminate the reverse recovery while achieving the

TABLE II
COMPONENTS OF THE EXPERIMENTAL DL//S ZCS-QRC

Fig. 1(f) Reference	VALUE
L_1	220 μH
L_r	10 μH
C_r	10 nF
S_1	FDMS86105

TABLE III
COMPONENTS OF THE EXPERIMENTAL DL//L ZCS-QRC

Fig. 5(a) Reference	VALUE
L_1	400 μH
L_r	4.7 μH
C_r	6.8 nF
S_1	FDMS86105

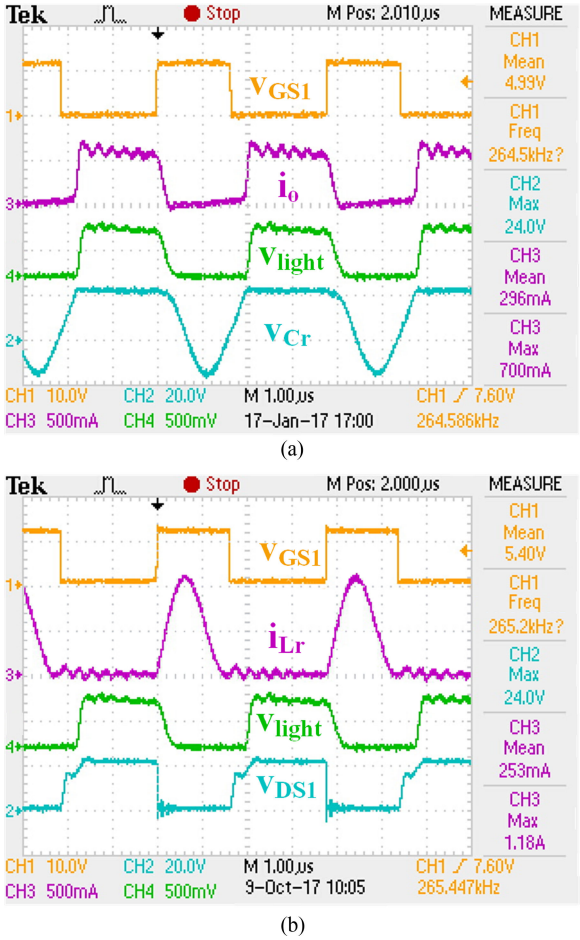

Fig. 11. Most representative waveforms for the DL//S ZCS-QRC. (a) Output current and reference waveforms. (b) Resonant current and reference waveforms.

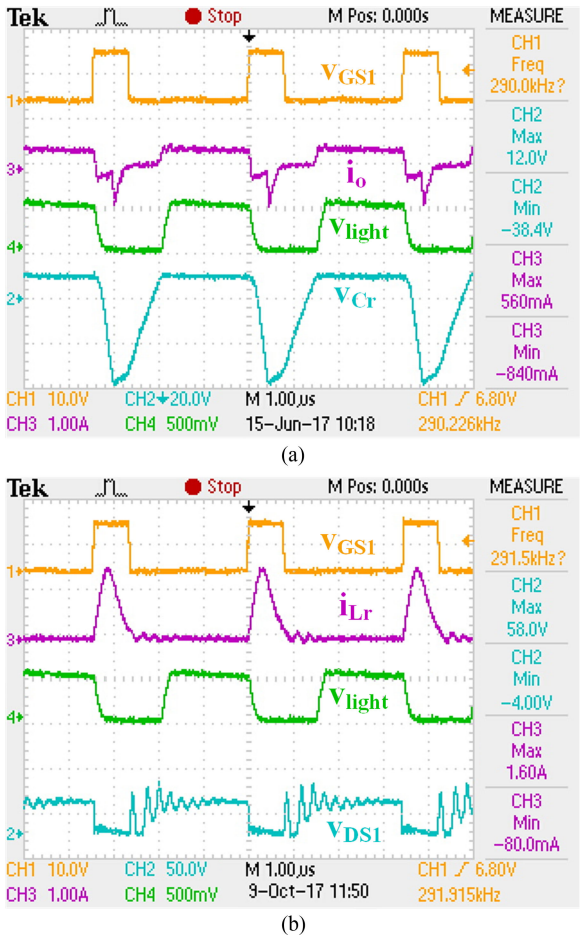

Fig. 12. Most representative waveforms for the DL//*L* ZCS-QRC. (a) Output current and reference waveforms. (b) Resonant current and reference waveforms.

ZCS condition. Moreover, the switching frequency of the HB-LED driver varies from 235 kHz at full dimming to 265 kHz at full load, being HB-LED1 from Table I the one used as both the rectifier and the load.

Depicted in Fig. 11(a) are the waveforms of the DL//S ZCS-QRC converter, which show no reverse recovery by adjusting the turn-off di/dt of $i_o(t)$ with an adequate value of L_r. Moreover, the converter achieves the ZCS condition as shown in Fig. 11(b). It should be noted that some ringing appears during the turn-on of the HB-LED string due to the conduction of the parasitic diode of S_1 at the end of the resonant stage.

B. Experimental Results for the DL//L ZCS-QRC

Following the same principle as the previous driver, the DL//*L* ZCS-QRC has been designed in order to eliminate the reverse recovery effect, while fulfilling the ZCS requirement. Its components have been summarized in Table III for an input voltage of 24 V feeding two strings of four HB-LEDs, which are equivalent to 12 V at 0.6 mA.

Fig. 12 shows the most representative waveforms for this driver. As can be seen in Fig. 12(a), $i_o(t)$ presents an undesired negative current peak in the middle of the turn-off of the HB-LED. Even though, this current peak does not have any impact in terms of the generated light, it will decrease both the lifetime and the luminous efficiency of the driver greatly. This peak happens due to the high reverse voltage, which causes a new unexpected stage to occur. In fact, as Fig. 12(b) shows, the driver is unable to achieve full ZCS due to this limitation.

A test over time has been done for the driver under study, in order to observe the implications of applying a negative voltage higher than the maximum forward voltage of the string in

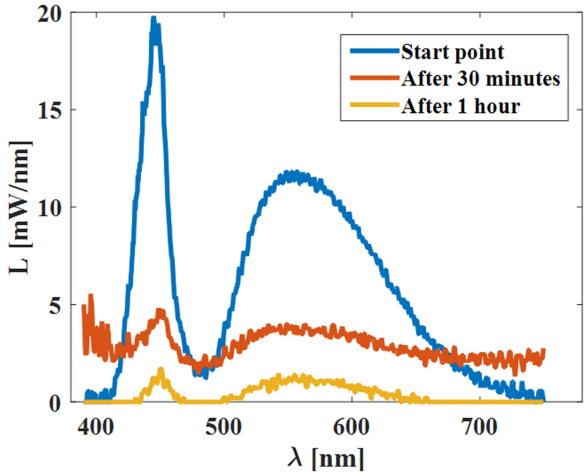

Fig. 13. Luminance versus wavelength in the visible spectrum for different time instants.

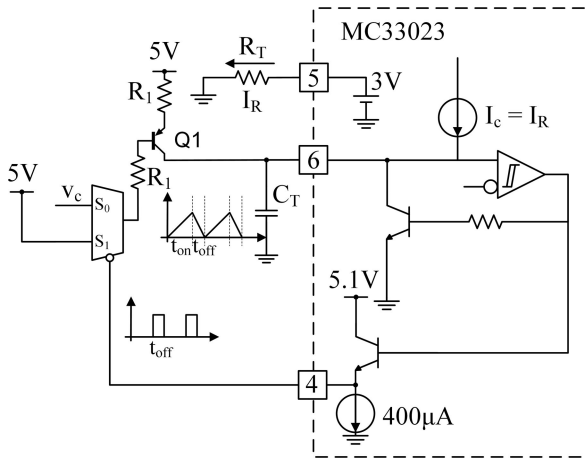

Fig. 14. External circuitry proposed to control the turn-off duration.

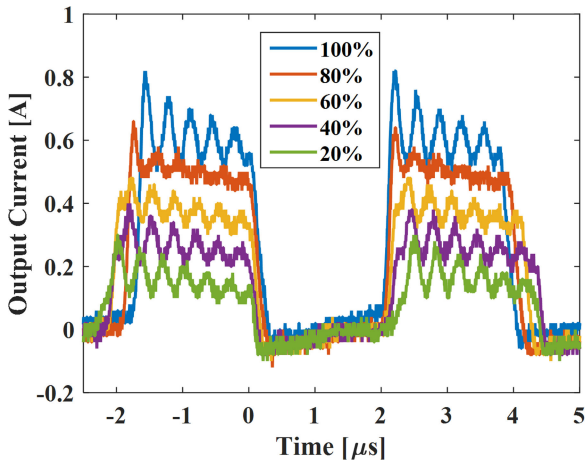

Fig. 15. Current across the LEDs in the DL//S ZCS-QRC for different dimming conditions.

terms of the light output provided by the HB-LEDs. Fig. 13 shows the measured luminance with the help of a spectrophotocolorimeter and an integrating sphere. As can be seen, in a time span of an hour, the HB-LED string is rendered useless due to the limitations of the reverse blocking capabilities of HB-LEDs. This limitation cannot be simply overcome without adding more components to the circuit, which will hinder the efficiency of the driver. Hence, the topology being discarded for driving HB-LEDs unable to block reverse voltages higher than their V_{γ_LED}.

C. Control Strategy

Before jumping into the reliability testing, the control of the DL//S ZCS-QRC needs to be discussed. In order to reduce the cost of the proposed converter to make it suitable for an application, a commercial analog integrated circuitry (IC) capable of switching up to 1 MHz is going to be used. The DL//S ZCS-QRC requires for its frequency to be controlled in order to regulate the output either in terms of current, or the light output [30]. Previous works have tackled this topic on ZCS-QRCs, by adding a simple external circuit to commercial ICs in order to have control over the off time [31]–[33].

Fig. 14 shows the proposed circuitry to control the driver. The idea is based on using a PNP bipolar junction transistor (BJT) in conjunction with the analog multiplexer to generate a precision controlled current source that is able to regulate the charge of C_T, which can be faster or slower depending on the output voltage of the compensator (v_c). The BJT will be working in the linear region taking into consideration its current source capabilities. Hence, changing its current source value depending on the voltage supplied by the control loop.

In order to keep a constant on-time, the BJT needs to work as a current source only during the OFF time. Hence, an analog multiplexer is used to switch OFF the bipolar transistor during t_{on} and switch it ON during t_{off}.

This circuit has been validated in open loop by controlling the driver switching frequency with an external power supply assuring that I_{in} and I_o follow the relationship introduced in (26) for the whole range of operation. It is important to note, that in the proposed driver the LEDs are dimmed by varying the frequency of the converter. By doing so, the average current lowers with the switching frequency. At the same time, the converter demands less power and the input current decreases, causing the current peak on the LEDs to decrease, which means that the ZCS condition is guaranteed during the whole operation of the LED driver in accordance to (48). Hence, by dimming the LEDs, the switching frequency and the current through the LEDs changes, see Fig. 15 for the DL//S ZCS-QRC. In fact, the variation of two different design parameters normally require a complicated control loop, however, in the case of study, the input current is dependent on the switching frequency, so only the switching frequency is required to be controlled through the control loop.

In order to study how to design the compensator, the open-loop gain of the DL//S ZCS-QRC has been measured by means of a Venable 6320. The results of these measurements are summarized in Fig. 16 for four different operating points (i.e., 100%, 80%, 50%, and 20% of the load), where it can be observed that the most restrictive condition is set at full load. Hence, a compensator has been designed to assure stability for all the range of operation with a crossover frequency of 10 kHz, a gain margin of 22.5 dB and a phase margin of 62°.

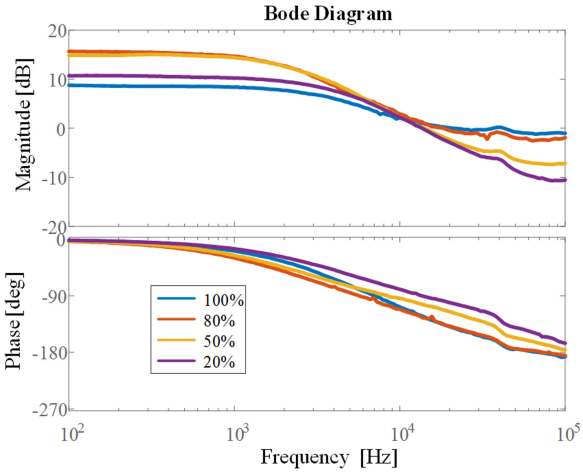

Fig. 16. Open-loop gain of the DL//S ZCS-QRC for different dimming conditions.

D. Comparison and Reliability Testing

As it was previously introduced in this section, the DL//S ZCS-QRC is going to be compared with a dc–dc boost converter, which requires an additional power diode and an output capacitor of 10 μF to diminish the current ripple, and a DL//S. The comparison will be done in terms of luminous efficacy, which will be measured in lm/W considering the losses of the control circuitry, and CCT. Even though, the electrical efficiency is not going to be compared, as the luminous efficacy makes for a fairer comparison between the drivers under study, the electrical efficiency for the DL//S ZCS-QRC is higher than the other two drivers achieving a 94.5% at full-load conditions, measured in open loop not considering the losses of the extra components used for closed loop operation (i.e., analog multiplexer, BJT, and operational amplifier for closed-loop operation).

The integrating sphere used in the testing is shown in Fig. 17, and it was used in conjunction with an spectrophotocolorimeter from LabSphere Inc. Fig. 18 shows a comparison between the three drivers for both luminous efficacy and CCT in terms of the output current for different dimming conditions. The measurements are normalized at the value of maximum output current measured on each driver to fairly compare the drivers behavior. As can be seen the DL//S ZCS-QRC presents less variation in luminous efficacy when varying the reference of the control loop to attain the different dimming conditions. It should be noted, that the CCT does not present significant variations as a function of i_o and that the dc–dc boost is the best in the aforementioned conditions.

For the reliability testing, 12 prototypes have been designed four for each driver under test, with two of drivers operating at 150 mA and the other two at 300 mA of average i_o for 700 h uninterruptedly. The measurements have been done in the integrating sphere every 175 h to exemplify the degradation behavior of each driver over time.

The experimental results in terms of luminous efficacy for the three drivers are summarized in Fig. 19(a) for 150 mA and (b) for 300 mA of average output current. As can be seen, the DL//S luminous efficacy plummets becoming irreversibly less

Fig. 17. Integrating sphere and spectrophotocolorimeter from LabSphere Inc. used for the measurements.

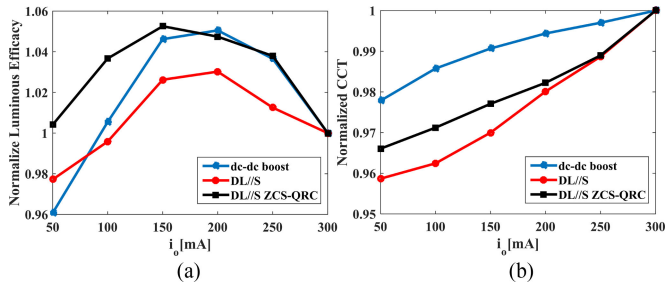

Fig. 18. Measurements for the three drivers under test. (a) Normalized luminous efficacy versus i_o. (b) Normalized CCT versus i_o.

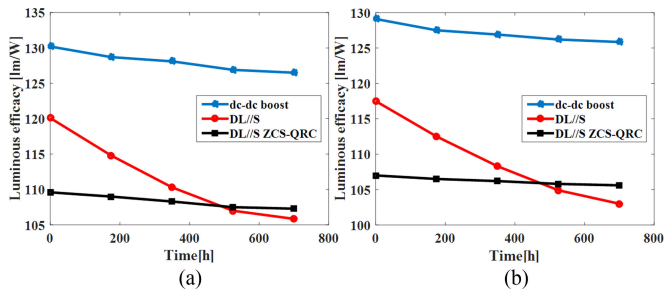

Fig. 19. Measurements for the three drivers under test. (a) Luminous efficacy at 150 mA versus time. (b) Luminous efficacy at 300 mA versus time.

efficient than the proposed converter in roughly 600 h due to the reverse-recovery effect, as it was assumed at the start of this section. In fact, the dc–dc boost degrades at a higher rate than the DL//S ZCS-QRC in both scenarios. This last fact, has been proved in other studies comparing dc and pulsed-current HB-LED driving, where the efficiency of the HB-LEDs would keep falling at a higher ratio on 3 000-h test [17]. Even though, the difference is not as high as for the DL//S, this fact will arguably

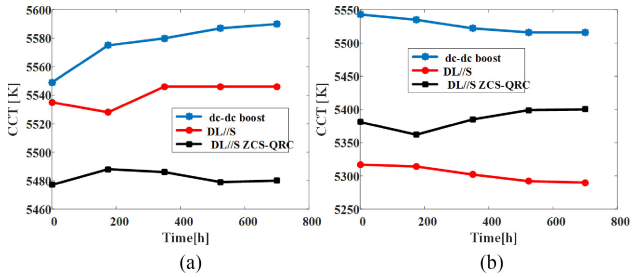

Fig. 20. Measurements for the three drivers under test. (a) CCT at 150 mA versus time. (b) CCT at 300 mA versus time.

make the proposed DL//S ZCS-QRC a solution able to achieve a longer lifespan than the conventional proposal. It should be noted that, at higher currents, the drivers degrade with a higher ratio, but it does not seem to be noticeable over the period of time that was studied. Furthermore, the difference in terms of luminous efficacy at the start of test between the DL//S and the DL//S ZCS-QRC can be explained due to the extra components required for the closed-loop operation, as the total power losses are considered in its determination. The difference between the dc–dc boost and the other two drivers were also expected as pulsed-current driving is less efficient than dc driving [17].

Finally, Fig. 20 shows that there is no relevant variation in terms of CCT over time for any of the drivers under study, under the two different current conditions.

IV. Conclusion

A family of ac-LED, ZCS-QRC, converters fed from dc voltages, which uses the HB-LEDs both as the rectifier diode and the load of the converter, switching at high frequencies has been presented. Moreover, both the DL//S ZCS-QRC and the DL//*L* ZCS-QRC have been designed and experimentally tested. The experimental results for the DL//S ZCS-QRC matches the predicted behavior of the theoretical analysis. However, the DL//*L* ZCS-QRC requires a higher blocking negative voltage on the HB-LEDs to avoid its reverse conduction, which makes it an inadequate solution for driving HB-LEDs.

In order to understand how well does the DL//S ZCS-QRC stand in comparison to a classic solution and the DL//S, several prototypes have been designed and constructed with closed-loop operation to assure the nonvariation of the average value of the output current. After a preliminary comparison that showed that the DL//S ZCS-QRC does have a lesser fluctuation in terms of luminous efficacy for different dimming conditions, all the prototypes were left working for 700 h with its HB-LEDs replaced with newer ones that had not been operated before. This last test showed that, even though, the DL//S ZCS-QRC initial luminous efficacy was the lowest, its degradation over time in terms of this parameter was the smallest being able to match that of the DL//S in a period of 500 h and arguably being able to do the same with the dc–dc boost over longer periods of time, if the tendency is kept the same for both drivers. This better performance in terms of its lifetime, the ability to remove the rectifier and diminishing the size of the output capacitor of the dc–dc boost, and the capability to reach higher frequencies due to the soft-switching operation make the DL//S ZCS-QRC an interesting solution for the high-frequency HB-LED driving as postregulators or as the interface between the HB-LEDs and the nanogrid.

References

[1] M. Arias, A. Vazquez, and J. Sebastian, "An overview of the AC-DC and DC-DC converters for LED lighting applications," *Automatika*, vol. 53, pp. 156–172, 2012.

[2] Y. Chen, C. Chang, and P. Yang, "A novel constant current control circuit for a primary-side controlled AC-DC LED driver," in *Proc. 11th Int. Conf. Electron., Comput. Comput.*, Abuja, Nigeria, 2014, pp. 1–4.

[3] J. Yang *et al.*, "A universal-input high-power-factor LLC resonant driver without electrolytic capacitor for PWM dimming LED lighting application," in *Proc. Int. Power Electron. Appl. Conf. Expo.*, Shanghai, China, 2014, pp. 1473–1478.

[4] *Electromagnetic Compatibility (EMC)—Part 3-2: Limits – Limits for Harmonic Current Emissions (Equipment Input Current < 16 A per Phase), IEC 61000-3-2*, 2014.

[5] Q. Hu and R. Zane, "Off-line LED driver with bidirectional second stage for reducing energy storage," in *Proc. IEEE Energy Convers. Congr. Expo.*, Phoenix, AZ, USA, 2011, pp. 2302–2309.

[6] C. Spini, *48 V-130 W High-Efficiency Converter With PFC for LED Street Lighting Applications*, STMicroelectronics, Appl. Note AN3106, pp. 1–34, 2012.

[7] M. Arias, D. G. Lamar, J. Sebastian, D. Balocco, and A. A. Diallo, "High-efficiency LED driver without electrolytic capacitor for street lighting," *IEEE Trans. Ind. Appl.*, vol. 49, no. 1, pp. 127–137, Jan./Feb. 2013.

[8] J. Sebastian, P. J. Villegas, F. Nuno, and M. M. Hernando, "High-efficiency and wide-bandwidth performance obtainable from a two-input buck converter," *IEEE Trans. Power Electron.*, vol. 13, no. 4, pp. 706–717, Jul. 1998.

[9] J. Sebastian, P. J. Villegas, F. Nuno, O. Garcia, and J. Arau, "Improving dynamic response of power-factor preregulators by using two-input high-efficient postregulators," *IEEE Trans. Power Electron.*, vol. 12, no. 6, pp. 1007–1016, Nov. 1997.

[10] M. Hernando, J. Sebastian, P. J. Villegas, and S. Ollero, "Improving dynamic response of power-factor correctors by using series-switching postregulator," *IEEE Trans. Ind. Electron.*, vol. 46, no. 3, pp. 563–568, Jun. 1999.

[11] B. G. Kang, Y. Choi and S. K. Chung, "High frequency AC-LED driving for street light," in *Proc. 9th Int. Conf. Power Electron, ECCE Asia*, Seoul, South Korea, 2015, pp. 1246–1251.

[12] C. L. Kuo, T. J. Liang, K. H. Chen, and J. F. Chen, "Design and implementation of high frequency AC-LED driver with digital dimming," in *Proc. IEEE Int. Symp. Circuits Syst.*, Paris, France, 2010, pp. 3713–3716.

[13] K. H. Loo, Y. M. Lai, and C. K. Tse, "Design and analysis of LCC resonant network for quasi-lossless current balancing in multistring AC-LED array," *IEEE Trans. Power Electron.*, vol. 28, no. 2, pp. 1047–1059, Feb. 2013.

[14] J. C. W. Lam and P. K. Jain, "A high power factor, electrolytic capacitor-less AC-input LED driver topology with high frequency pulsating output current," *IEEE Trans. Power Electron.*, vol. 30, no. 2, pp. 943–955, Feb. 2015.

[15] M. A. Juárez, P. R. Martínez, G. Vázquez, J. M. Sosa, and M. Ponce, "Analysis and design for self-oscillating LED driver with high frequency pulsating output current," in *Proc. 41st Annu. Conf. IEEE Ind. Electron. Soc.*, Yokohama, Japan, 2015, pp. 003992–003996.

[16] W. Feng, Y. He, and F. G. Shi, "Investigation of LED light output performance characteristics under different alternating current regulation modes," *IEEE J. Sel. Topics Quantum Electron.*, vol. 17, no. 3, pp. 720–723, May/Jun. 2011.

[17] J. Zhou and W. Yan, "Experimental investigation on the performance characteristics of white LEDs used in illumination application," in *Proc. IEEE Power Electron. Spec. Conf.*, Orlando, FL, USA, 2007, pp. 1436–1440.

[18] M. S. Lin and C. L. Chen, "An LED driver with pulse current driving technique," *IEEE Trans. Power Electron.*, vol. 27, no. 11, pp. 4594–4601, Nov. 2012.

[19] J. P. You *et al.*, "Phosphor-concentration-dependent characteristics of white LEDs in different current regulation modes." *J. Electron. Mater.*, vol. 38, no. 6, 2009, pp. 761–766.

[20] *IEEE Recommended Practices for Modulating Current in High-Brightness LEDs for Mitigating Health Risks to Viewers, IEEE Std. 1789-2015*, pp. 1–80, Jun. 5, 2015.
[21] J. Sebastian, D. G. Aller, J. Rodríguez, D. G. Lamar, and P. F. Miaja, "On the role of the power electronics on visible light communication," in *Proc. IEEE Appl. Power Electron. Conf. Expo.*, Tampa, FL, USA, 2017, pp. 2420–2427.
[22] P. Haaf and J. Harper, "Understanding diode reverse recovery and its effect on switching losses," 2007. [Online]. Available: https://www.fairchildsemi.com/technical-articles/Understanding-DiodeReverse-Recovery-and-Its-Effect-on-Switching-Losses.pdf
[23] M. M. Jovanovic, "A technique for reducing rectifier reverse-recovery-related losses in high-power boost converters," *IEEE Trans. Power Electron.*, vol. 13, no. 5, pp. 932–941, Sep. 1998.
[24] F. C. Lee, "High-frequency quasi-resonant converter technologies," *Proc. IEEE*, vol. 76, no. 4, pp. 377–390, Apr. 1988.
[25] S. Freeland and R. D. Middlebrook, "A unified analysis of converters with resonant switches," in *Proc. IEEE Power Electron. Spec. Conf.*, Blacksburg, VA, USA, 1987, pp. 20–30.
[26] K. H. Liu, R. Oruganti, and F. C. Y. Lee, "Quasi-resonant converters-topologies and characteristics," *IEEE Trans. Power Electron.*, vol. PE-2, no. 1, pp. 62–71, Jan. 1987.
[27] A. F. Witulski and R. W. Erickson, "Extension of state-space averaging to resonant switches and beyond," *IEEE Trans. Power Electron.*, vol. 5, no. 1, pp. 98–109, Jan. 1990.
[28] D. Boroyevich, I. Cvetković, D. Dong, R. Burgos, F. Wang, and F. Lee, "Future electronic power distribution systems a contemplative view," in *Proc. 12th Int. Conf. Optim. Elect. Electron. Equip.*, Basov, Romania, 2010, pp. 1369–1380.
[29] *Cree XLamp LED Electrical Overstress*, Cree, Inc., Durham, NC, USA, Appl. Note CLD-AP29 REV 1E, 2016.
[30] X. Zhan, H. Chung, and R. Zhang, "Investigation into the use of single inductor for driving multiple series-connected LED channels," *IEEE Trans. Power Electron.*, vol. 32, no. 4, pp. 3034–3050, Apr. 2017.
[31] J. Sebastian *et al.*, "Aspectos tecnológicos en el diseño de convertidores cc/cc resonantes: Circuitos de mando," (in Spanish), *Mundo Electrónico*, no. 196, pp. 92–98, 1989.
[32] M. A. Perez *et al.*, "Design of a power supply system based on two quasi-resonant converters," *Eur. Space Power Conf.*, vol. 294, 1989, pp. 345–350.
[33] I. Castro, S. Lopez, K. Martin, M. Arias, D. G. Lamar, and J. Sebastian, "High frequency dc-dc AC-LED driver based on ZCS-QRCs," in *Proc. IEEE Energy Convers. Congr. Expo.*, Cincinnati, OH, USA, 2017, pp. 3688–3695.

Ignacio Castro (S'14) was born in Gijón, Spain, in 1989. He received the M.Sc. degree in telecommunication engineering from the University of Oviedo, Gijón, in 2014, where he is currently working toward the Ph.D. degree in electrical engineering.

His research interests include low- and medium-power dc–dc converters, modeling, simulation, and control of dc–dc converters, power-factor correction ac–dc converters, and light-emitting-diode drivers.

Diego G. Lamar (S'05–M'08) was born in Zaragoza, Spain, in 1974. He received the M.Sc. and Ph.D. degrees in electrical engineering from the Universidad de Oviedo, Gijón, Spain, in 2003 and 2008, respectively.

In 2003 and 2005, he became a Research Engineer and an Assistant Professor, respectively, with the University of Oviedo. Since September 2011, he has been an Associate Professor. His research interests include switching-mode power supplies, converter modeling, and power-factor-correction converters.

Sergio Lopez was born in Oviedo, Spain, in 1994. He received the Bachelor of Engineering degree in telecommunication from the University of Oviedo, Gijón, Spain, in 2016, where he is currently working toward the Master degree in telecommunications engineering.

His research interests include power electronics, signal processing, and radio-frequency and microwave technologies.

Kevin Martin (S'13) was born in Gijón, Spain, in 1990. He received the M.Sc. degree in telecommunication engineering from the University in Oviedo, Gijón, in 2014, where he is currently working toward the Ph.D. degree in electrical engineering on dc–dc power converters optimization and integration within dc microgrids.

Since 2014, he has been a Researcher with the Power Supply System Group, University of Oviedo. His research interests include dc–dc power supplies, modeling, simulation, and control of dc–dc power converters, and the use of wide bandgap semiconductor devices.

Manuel Arias (S'05–M'10) received the M. Sc. degree in electrical engineering and the Ph.D. degree in electrical engineering from the University of Oviedo, Gijón, Spain, in 2005 and 2010, respectively.

In 2007, he joined the University of Oviedo as an Assistant Professor, and since 2016, he has been an Associate Professor. His research interests include ac–dc and dc–dc power converters, battery-cell equalizers, and light-emitting-diode lighting.

Javier Sebastian (M'87–SM'11) was born in Madrid, Spain, in 1958. He received the M.Sc. degree in electrical engineering from the Technical University of Madrid (UPM), Madrid, in 1981, and the Ph.D. degree in electrical engineering from the University of Oviedo, Oviedo, Spain, in 1985.

He was an Assistant Professor and an Associate Professor at both the UPM and the University of Oviedo. Since 1992, he has been with the University of Oviedo, where he is currently a Professor. His research interests include switching-mode power supplies, modeling of dc-to-dc converters, low output voltage dc-to-dc converters, high power factor rectifiers, light-emitting-diode drivers, dc-to-dc converters for envelope tracking techniques, and the use of wide bandgap semiconductors in power supplies.